doi: 10.37905/jgeosrev.v8i1.34364 ejurnal.ung.ac.id/index.php/jgeosrev

Vol. 8, No. 1, January 2026: 108-119

Jambura Geoscience Review

p-ISSN 2623-0682 | e-ISSN 2656-0380

Department of Earth Science and Technology, Universitas Negeri Gorontalo

# Geochemical Characteristics of Basalt in the Northern Taopa Area, Parigi Moutong Regency, Central Sulawesi

Sri Wanda Magfira[1], Asrafil[1], Riska Puspita[1]

[1]*Geological Engineering Study Program, Tadulako University, Jl. Soekarno Hatta, Palu, Central Sulawesi, 94148, Indonesia*

**ARTICLE INFO**

**Article history:**
Received: 9 September 2025
Accepted: 24 December 2025
Published: 15 January 2026

**Keywords:**
Basalt; Central Sulawesi; Geochemistry
Ocean island tholeiite (OIT); Taopa

**Corresponding author:**
Sri Wanda Magfira
Email:
sriwandamagfira1608@gmail.com

**Read online:**
Scan this QR code with your smart phone or mobile device to read online.

**ABSTRACT**

This study analyzes the geochemical characteristics of basaltic rocks in the Northern Taopa (Taopa Utara) area, Parigi Moutong Regency, Central Sulawesi, to constrain magma affinity, magmatic series, and tectonomagmatic setting. Although Central Sulawesi records complex arc–oceanic interaction, the major-element geochemistry of basalts from Northern Taopa has remained poorly documented. Petrographic observations and X-ray fluorescence (XRF) major-oxide analyses were conducted on four representative samples (ST10, ST19, ST24, and ST36). Petrographic analysis shows that all samples have a hypocrystalline–porphyritic texture with plagioclase, clinopyroxene, olivine, and opaque minerals set in a microlitic groundmass. Major-oxide compositions are characterized by SiO2 48.85–50.65 wt% and total Fe2O3 12.89–13.11 wt%, consistent with mafic basalt. On the total alkali–silica diagram the samples plot in the basalt field and display low total alkalis (Na2O+K2O 1.11–2.11 wt%) and very low K2O (0.039–0.051 wt%), indicating a low-K subalkaline affinity. AFM relations show relative Fe enrichment and place the samples within the tholeiitic series. Tectonic discrimination using TiO2–P2O5–MnO (TiO2 0.98–1.06 wt%; P2O5 0.405–0.427 wt%; MnO 0.208–0.276 wt%) suggests an ocean-island tholeiite (OIT) signature. The low-K tholeiitic, OIT-like character implies an intraplate oceanic mantle source contribution to basalt generation and provides quantitative constraints for refining regional tectonic reconstructions of Central Sulawesi during emplacement of the Taopa volcanic unit.

**How to cite:** Magfira, SW. (2026). Geochemical Characteristics of Basalt in the Northern Taopa Area, Parigi Moutong Regency, Central Sulawesi. *Jambura Geoscience Review, 8*(1), 108-119. https://doi.org/10.37905/jgeosrev.v8i1.34364

## 1. INTRODUCTION

Sulawesi Island is divided into four major geological mandalas, one of which is the West and North Sulawesi Volcanic–Plutonic Arc (Hall & Wilson, 2000). This arc represents a key segment of the Indonesian tectonic framework and records long-lived magmatic activity related to complex plate interaction. The northern segment of the arc is dominated by rhyodacitic to andesitic volcanic rocks formed during the Miocene–Recent period, underlain by an older basaltic basement of Eocene–Oligocene age. In contrast, the western segment is characterized by continental-affinity rocks consisting of Mesozoic–Quaternary volcanic units and ancient Mali rocks of Cretaceous age (Sompotan, 2012; Zhang et al., 2024)).

Regionally, northern Sulawesi has a complex tectonic configuration involving multiple subduction systems and large strike-slip fault zones. The interaction between the North Sulawesi Subduction Zone, the East Sangihe Subduction Zone, and major structures such as the Palu–Koro and Balantak faults has exerted strong control on magmatic evolution from the Tertiary to the Quaternary, resulting in widespread volcanic activity across Central Sulawesi (Surono & Hartono,

2013 Cao et al., 2024; Song et al., 2022; Simanjuntak et al., 2024). Therefore, understanding the geochemical characteristics of volcanic rocks within this framework is essential for reconstructing regional tectonomagmatic processes.

Within this regional context, basaltic rocks represent an important record of mantle-derived magmatism and tectonic settings. However, the genetic interpretation of basalts relies heavily on robust petrographic observations and quantitative geochemical data, particularly major element compositions that constrain magma affinity and magmatic series (Takaew et al., 2024; Zhang et al., 2022; Godang et al., 2025. In many parts of Central Sulawesi, such data are unevenly distributed and locally incomplete.

The general approach to address this problem involves the integration of petrographic analysis with whole-rock major-element geochemistry, which together provide a fundamental basis for classifying basalt types, identifying magmatic series, and inferring tectonomagmatic environments. This combined methodology has been widely applied in volcanic terranes to discriminate between arc-related, intraplate, and mid-ocean ridge basaltic affinities (Doucet et al., 2022; Nakamura, 2023; Park et al., 2022).

Previous studies have demonstrated that petrographic characteristics, such as mineral assemblages and textures, provide initial constraints on magma evolution and crystallization history, whereas major element geochemical data enable the quantitative classification of basaltic rocks. Diagrams such as the Total Alkali–silica (TAS) and AFM plots are commonly used to evaluate magma affinity and differentiation trends, forming a standard framework in igneous petrology (Oggier et al., 2023; Vermeesch & Pease, 2021).

In addition, tectonomagmatic discrimination based on major oxides has proven to be effective in distinguishing basalt sources and settings. Geochemical discrimination diagrams employing $TiO_2$, $P_2O_5$, and MnO have been widely applied to infer oceanic, arc-related, and intraplate basalt signatures, particularly in regions with complex tectonic histories similar to that of Sulawesi.

These approaches provide a clear methodological pathway for investigating basalt genesis. Applying such standardized petrographic and geochemical frameworks to understudied volcanic units allows local datasets to be placed within a broader regional and global context, thereby enhancing their interpretive value.

Despite the extensive application of petrographic and geochemical methods in many volcanic provinces, site-specific and systematically documented geochemical studies of basaltic rocks from the Northern Taopa area are scarce. Existing regional geological maps describe the presence of basalt within the volcanic rock unit (Ttv) however, detailed major element geochemical datasets required to rigorously constrain the magma affinity, magmatic series, and tectonic setting are largely unavailable in the published literature (Ratman, 1976).

Consequently, the role of Northern Taopa basalts in the broader tectonomagmatic evolution of Central Sulawesi has not been adequately evaluated, representing a clear knowledge gap compared to better-studied basaltic occurrences elsewhere on the island.

The objective of this study is to determine the petrographic characteristics and major-element geochemical composition of basaltic rocks from the Northern Taopa area to identify their magma affinity and tectonomagmatic setting. The study focuses on integrated petrographic analysis and X-ray fluorescence (XRF) major-oxide geochemistry of representative basalt samples. This research provides the first quantitative major-element geochemical dataset for Northern Taopa basalts, establishing a baseline that contributes new constraints on basalt petrogenesis and regional magmatic evolution in Central Sulawesi.

## 2. METHOD

### 2.1. Study Area and Regional Geological Setting

Figure 1 shows the local spatial framework of the Taopa Utara research area and supports the documentation of outcrop distribution and sampling coverage. The local-scale position of the study area was interpreted within a broader stratigraphic and tectonic context using a regional geological map (Figure 2), which depicts the distribution of major lithostratigraphic units and structures surrounding Taopa Utara.

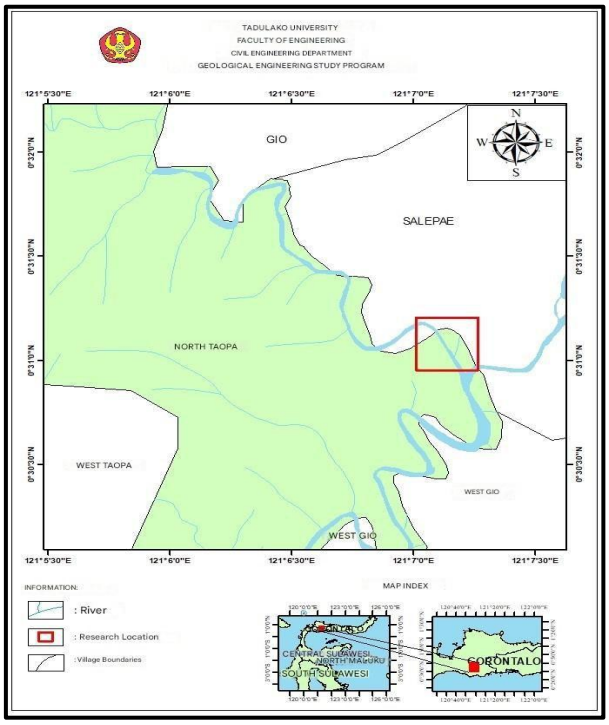


**Figure 1.** Map of the research area in the Taopa Utara region

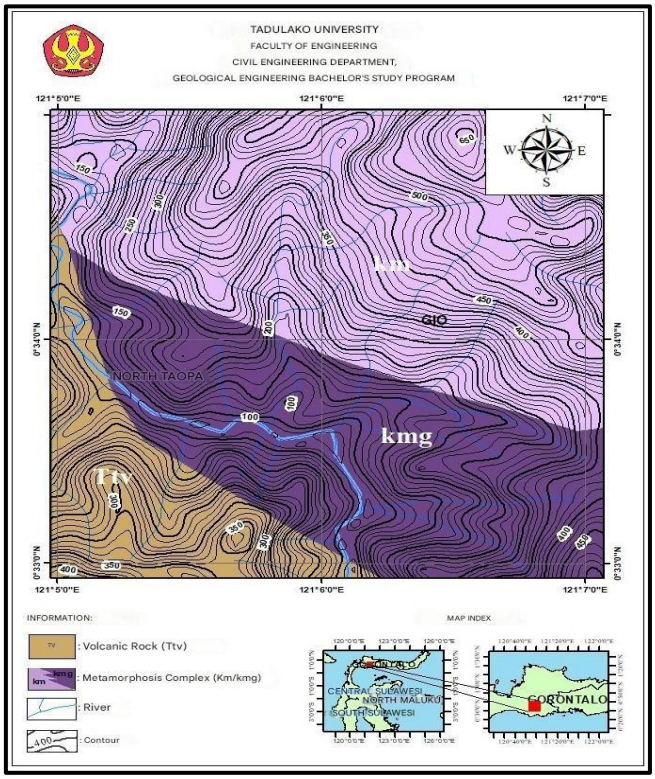


**Figure 2.** Regional geological map of the study area (Ratman, 1976)

## 2.2. Field Sampling

Field data collection involved geological mapping and observation of basalt outcrops in Taopa Utara, Indonesia. Sampling focused on fresh, minimally weathered basalt exposures to minimize alteration effects on the major element composition. Four basalt samples (ST10, ST19, ST24, and ST36) were collected to represent the basalt distribution in the study area. Sampling points were documented using field notes and GPS.

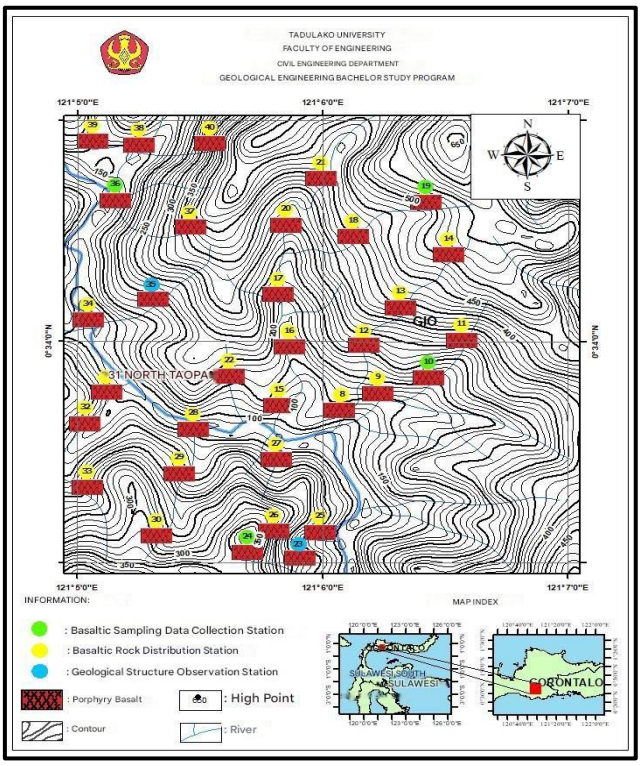


**Figure 3.** Map of observation stations and basalt sampling locations in the Taopa Utara area

### 2.3. Petrography

Petrographic analysis was conducted to determine the mineral assemblages and textures of the basalt samples. Representative chips from each sample were prepared as standard thin sections (thickness ≈ 30 μm). Thin sections were examined using a polarizing microscope under plane-polarized light (PPL) and cross-polarized light (XPL) illumination. Mineral identification, textural description, and qualitative modal estimation were consistently carried out for all samples to support the interpretation of crystallization history and magma evolution.

### 2.4. XRF Preparation and Analytical Settings

For chemical analysis, rock samples were prepared by crushing and grinding them into a homogeneous powder. Prior to pulverization, weathered rinds were removed, and only fresh interiors were processed. Powdered samples were homogenized and prepared following the Integrated Laboratory XRF protocol for major oxide analysis.

Geochemical analysis was performed at the Integrated Laboratory using X-ray fluorescence (XRF). The instrument was operated under laboratory-standard conditions for major oxides, with calibration performed using certified reference materials and routine quality control (standards, blanks, and duplicate checks) to ensure analytical consistency. The major oxides determined were $SiO_2$, $Al_2O_3$, $Fe_2O_3$(total), MgO, CaO, $Na_2O$, $K_2O$, $TiO_2$

### 2.5. Data Treatment and Normalization

Raw XRF outputs were compiled and screened prior to interpretation. Major oxide totals were checked for internal consistency, and data were recalculated to 100 wt% (anhydrous basis) to reduce the influence of volatiles and minor analytical drift. Iron was treated as total $Fe_2O_3$ in reporting, and where required for specific classification plots, Fe was handled consistently as total iron for comparative purposes across the samples. Only datasets passing the basic quality screening (reasonable totals and coherence with petrographic observations) were used for plotting and interpretation.

### 2.6. Diagram Plotting and Interpretation

Processed major element data were used to classify rock types and infer magma affinity, magmatic series, and tectonomagmatic settings. Rock classification was performed using the Total Alkali–silica (TAS) approach (Le Bas et al., 1986). Magma series trends were evaluated using AFM relations, and the tectonic environment was interpreted using $TiO_2$–$P_2O_5$–MnO discrimination diagrams.

Although the number of samples analyzed in this study was limited, the integration of petrographic observations, major element geochemical data, and regional geological context provides a coherent basis for interpreting basalt genesis and tectonomagmatic implications for the Taopa Utara area.

## 3. RESULTS AND DISCUSSION

### 3.1. Petrography

The basaltic rocks analyzed in this study consisted of four representative fresh samples (ST 10, ST 19, ST 24, and ST 36). Macroscopically, the hand specimens showed a fine-grained texture, dark gray to black color, and a mafic-dominated appearance; the dominant visible phases were consistent with plagioclase phenocrysts and mafic minerals (clinopyroxene ± olivine), rather than biotite.

Microscopically, all samples display hypocrystalline–porphyritic textures with subhedral to anhedral crystal habits, inequigranular relationships, and locally developed flow structures. The mineral composition is dominated by plagioclase, occurring as phenocrysts and microlites in the groundmass (albite to albite–calcic twinning). Clinopyroxene was identified as diopside in samples ST 10, ST 19, and ST 36, whereas sample ST 24 contained augite. Olivine occurs as a primary mafic phase with partially altered rims, and opaque minerals occur as small inclusions. The groundmass is dominated by microcrystalline plagioclase, indicating rapid cooling during the final stage of solidification. Overall, the petrographic assemblage is consistent with basaltic lava crystallization under relatively rapid cooling conditions, producing a microlitic groundmass around earlier-formed phenocrysts.

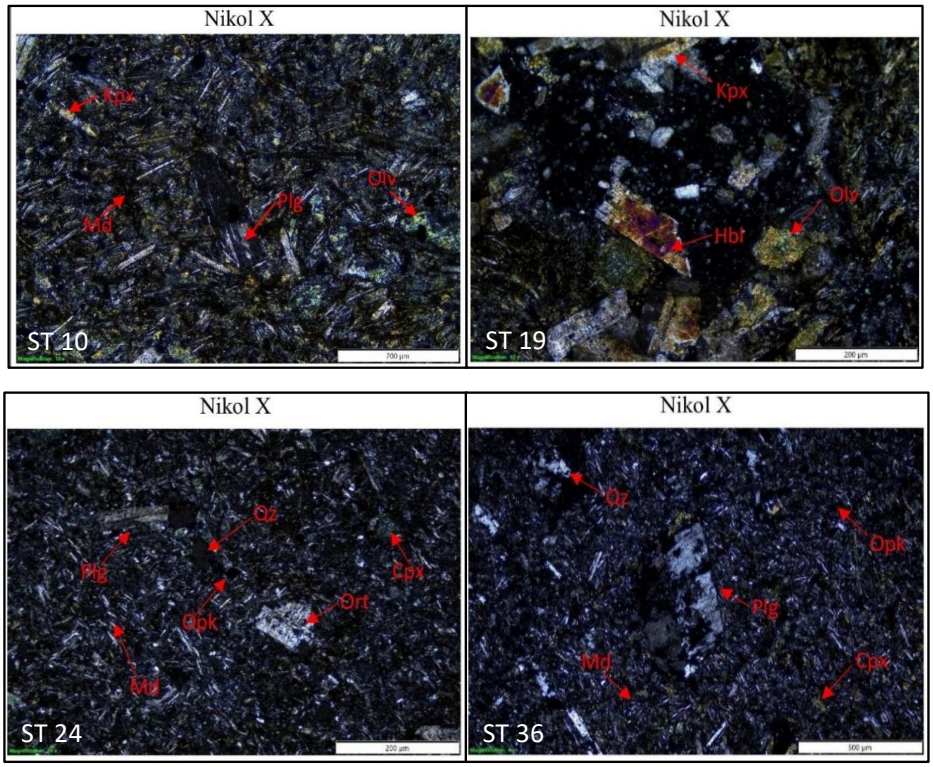


**Figure 4.** Appearance of the petrographic analysis results under cross-polarized light showing Basalt Porphyry (Travis, 1955).

The observed hypocrystalline–porphyritic fabric is characteristic of basaltic systems that experience a two-stage cooling history, that is, phenocryst growth at depth followed by rapid quenching during emplacement. The presence of plagioclase + clinopyroxene ± olivine, together with abundant microlites, is typical of basaltic lavas and supports the interpretation that the samples represent relatively mafic melts with limited silica evolution. Such mineralogical constraints are critical because they provide an independent check on geochemical classification outcomes, reducing the ambiguity in rock naming and magma-series assignment.

These petrographic characteristics indicate that the magma underwent two stages of crystallization: the formation of phenocrysts at depth before rapid solidification when the magma reached the surface. These characteristics directly support subsequent geochemical interpretations that require the early crystallization of Ca-bearing plagioclase and mafic phases. Accordingly, petrography provides the first line of evidence that the geochemical signatures discussed below reflect magmatic processes (fractional crystallization and differentiation) rather than being dominated by secondary overprinting.

### 3.2. Major Oxide Geochemistry

Geochemical analysis was carried out on 4 (four) basalt rock samples using X-ray fluorescence (XRF) to obtain the major oxide composition. The resulting data were then included as a comparison in analyses that covered rock type determination, magma affinity, magma series, and tectonic environment. The geochemical data are presented in Table 1.

**Table 1.** XRF analysis results of major oxide elements in basaltic rocks in the North Taopa Area

| Contents Main Oxides | Rock Sample (%) | | | |
|---|---|---|---|---|
| | ST 10 | ST 19 | ST24 | ST36 |
| $SiO_2$ | 50,646 | 48,847 | 49,302 | 50,157 |
| $Al_2O_3$ | 16,646 | 17,884 | 17,734 | 17,570 |
| MgO | 15,561 | 15,647 | 16,605 | 15,176 |
| $Fe_2O_3$ | 12,901 | 13,106 | 13,006 | 12,890 |
| $Na_2O$ | 1,851 | 2,058 | 1,057 | 1,679 |
| CaO | 0,604 | 0,600 | 0,567 | 0,670 |
| $K_2O$ | 0,04567 | 0,04789 | 0,05053 | 0,03924 |
| $TiO_2$ | 1,016 | 1,056 | 0,976 | 1,052 |
| $P_2O_5$ | 0,410 | 0,405 | 0,423 | 0,427 |
| MnO | 0,238 | 0,276 | 0,208 | 0,256 |

Based on Table 1, the four North Taopa samples are compositionally consistent with mafic basalt, with a narrow silica range ($SiO_2$ = 48.85–50.65 wt%) and moderate $Al_2O_3$ (16.65–17.88 wt%), while showing relatively high MgO (15.18–16.61 wt%) and elevated $Fe_2O_3$(total) (12.89–13.11 wt%), a combination that supports the tholeiitic basalt character. The rocks are also distinctly alkali-poor ($Na_2O$ = 1.06–2.06 wt%, $K_2O$ = 0.039–0.051 wt%, $Na_2O+K_2O \approx$ 1.11–2.11 wt%) with consistent ranges in other major oxides ($TiO_2$ ~0.98–1.06 wt%, $P_2O_5$ ~0.405–0.427 wt%, MnO ~0.208–0.276 wt%). The most notable feature is the exceptionally low CaO (0.567–0.670 wt%), indicating strong Ca depletion, which is most plausibly linked to early and/or extensive crystallization and separation of Ca-rich plagioclase and/or additional modification affecting Ca-bearing.

For basaltic rocks, the major element ranges of $SiO_2$ (~45–52 wt%) and $Al_2O_3$ (~13–17 wt%) are broadly consistent with common basalt compositions, whereas the combination of high MgO (15–16 wt%) and relatively high total iron ($Fe_2O_3$(total) ~13 wt%) supports a mafic, comparatively primitive character (Le Bas et al., 1986; Winter, 2014). In contrast, CaO is anomalously low relative to typical mafic basalt ranges; this deviation is substantial and therefore requires a process-based explanation rather than being treated as an analytical scatter.

CaO depletion is most plausibly explained by the early and effective removal of Ca-rich plagioclase during fractional crystallization, which is consistent with petrographic evidence of abundant plagioclase phenocrysts and plagioclase-rich microlitic groundmass (Winter, 2014). Because plagioclase preferentially partitions Ca, its early crystallization and separation from the

melt can drastically lower CaO in the residual liquid, while leaving $SiO_2$ in the basaltic range and maintaining low $K_2O$ in low-K systems.

The coexistence of (i) high MgO, (ii) elevated $Fe_2O_3$(total), (iii) very low alkalis, and (iv) anomalously low CaO indicates that the North Taopa basalts record a magmatic differentiation pathway dominated by early plagioclase control and continued crystallization of mafic phases. This geochemical pattern, when integrated with RD1 petrography, strengthens the confidence that subsequent diagram-based interpretations (TAS, AFM, and tectonic discrimination) reflect coherent magmatic evolution rather than inconsistent datasets.

### 3.3. Rock Type Classification

Rock-type determination based on total alkalis versus silica places all samples within the basalt field on the TAS diagram. The plotting results of this TAS diagram also correlate with the results of the petrographic analysis, which indicates porphyritic basalt, consistent with the geochemical analysis that also indicates basalt (Le Bas et al., 1986).

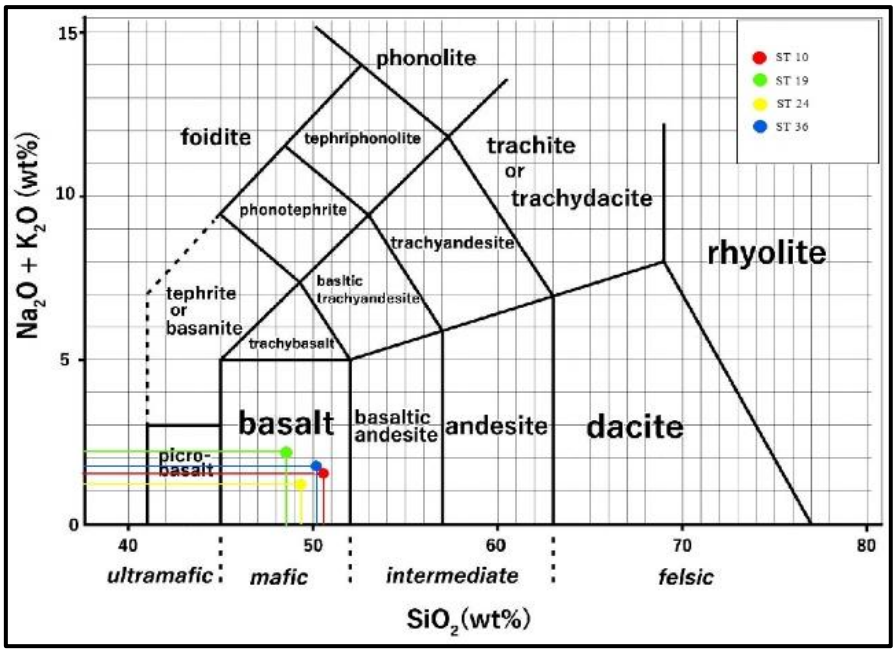


**Figure 5.** The plotting results comparing the content of SiO2 vs Na2O+K2O, based on the TAS diagram (Le Bas et al., 1986), indicate that the rock type is Basalt

The agreement between the TAS-based classification and petrographic identification is important because TAS fields can be influenced by the alteration or mobility of alkalis in some settings. Here, the alkalis are consistently low across all samples, and the petrographic assemblage (plagioclase + clinopyroxene ± olivine) supports a basalt classification, reducing the likelihood of misclassification driven by post-magmatic modifications (Bas et al., 1986; Lang et al., 2023; Pereira et al., 2024; Wu et al., 2021)).

This convergence between petrographic evidence and TAS-based classification establishes a robust baseline that the studied unit represents basaltic magma products and therefore justifies applying basalt-specific discriminants for magma-series determination and tectonomagmatic interpretation in subsequent analyses (Doucet et al., 2022; Marfian et al., 2023; Paputungan et al., 2025). Consequently, interpretations of low-K tholeiitic affinity and an OIT-related setting can be made on a consistent and internally validated compositional foundation.

### 3.4. Magma Affinity And Magma Series

Based on the plotting of $SiO_2$ values (48–50.6%) against $K_2O$ values (0.03–0.05%) in the magma affinity classification diagram (Peccerillo & Taylor, 1976), the plotting results indicate that the rocks in samples ST 10, ST 19, ST 24, and ST 36 from the research area are basalts with a tholeiitic (Low K) affinity.

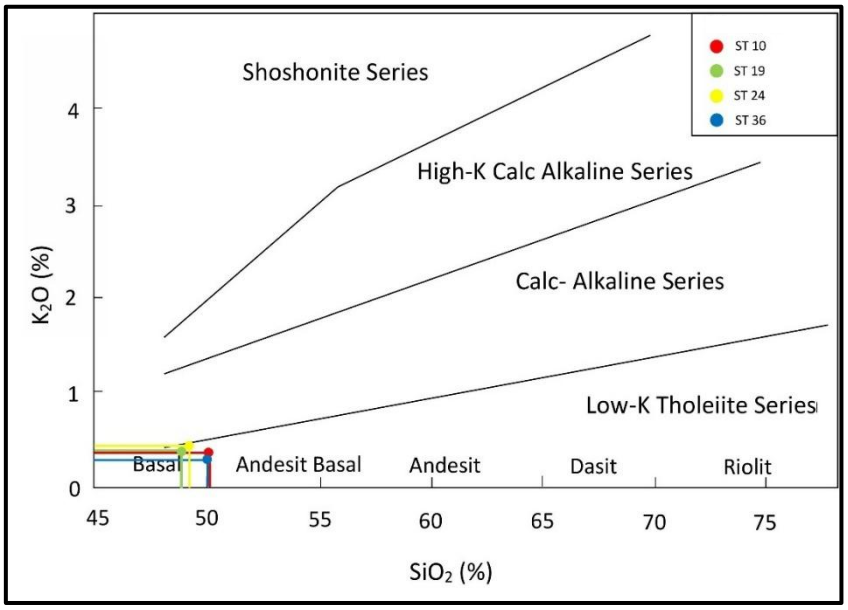


**Figure 6.** Magma affinity of basaltic rocks in the Taopa Utara area based on the Diagram (Peccerillo & Taylor, 1976)

The magma series of basaltic rock samples in the research area belongs to the tholeiitic series, which was analyzed based on a comparison of the percentage values of $Fe_2O_3$, MgO, and $Na_2O$ + $K_2O$ content after normalization to 100% on the AFM diagram (Irvine & Baragar, 1971).

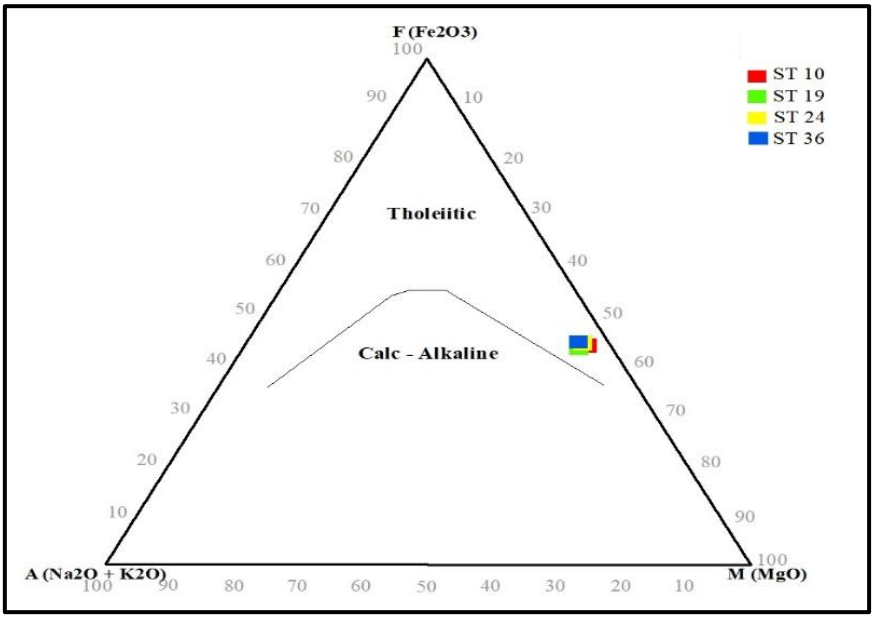


**Figure 7.** Plotting Results On The Magma Series Diagram (AFM) (Irvine And Baragar, 1971)

A defining feature of tholeiitic differentiation is Fe-enrichment relative to Mg during crystallization, which is commonly produced when mafic phases (notably olivine ± clinopyroxene) are removed while Fe remains comparatively elevated in the evolving melt prior to late-stage Fe–Ti oxide control (Winter, 2014; Irvine & Baragar, 1971). The major element pattern of this study —high total Fe together with high MgO and low alkalis—fits a low-K tholeiitic lineage and is consistent with the AFM tholeiitic trend.

Low $K_2O$ (≈0.04–0.05 wt%) further supports a low-K tholeiitic affinity and argues against strongly potassic or calc-alkaline enrichment, which typically presents higher K at comparable $SiO_2$ (Peccerillo & Taylor, 1976). Therefore, the combined evidence from the $SiO_2$–$K_2O$ and AFM diagrams provides a tighter and more defensible basis for the tholeiitic interpretation than relying on a single classification plot.

The identification of low-K tholeiitic basalts provides a critical link between the measured major element composition and inferred tectonomagmatic setting because tholeiitic basalts can form in more than one geodynamic environment and therefore require internally consistent process-based explanations (i.e., fractional crystallization pathways and mantle source characteristics) (Vermeesch & Pease, 2021). When combined with the petrographic evidence, the tholeiitic interpretation indicates a magma that remained alkali-poor during differentiation and developed Fe-enrichment characteristics of tholeiitic evolution, thereby strengthening the interpretation of an intraplate tholeiitic basalt component rather than an arc-related calc-alkaline series (Vermeesch & Pease, 2021; Marfian et al., 2023). This integrated petrographic-to-geochemical reasoning is consistent with regional igneous studies that couple field/petrographic constraints with laboratory data to support genetic interpretation (Rasyid et al., 2022).

### 3.5. Tectonic Environment

The analysis to determine the tectonic environment of rock formation was based on a magma source classification diagram (Mullen, 1983) and interpreted based on normalized $TiO_2$–MnO–$P_2O_5$ proportions (to 100%). The plotting results indicate an Oceanic Island Tholeiite (OIT) affinity.

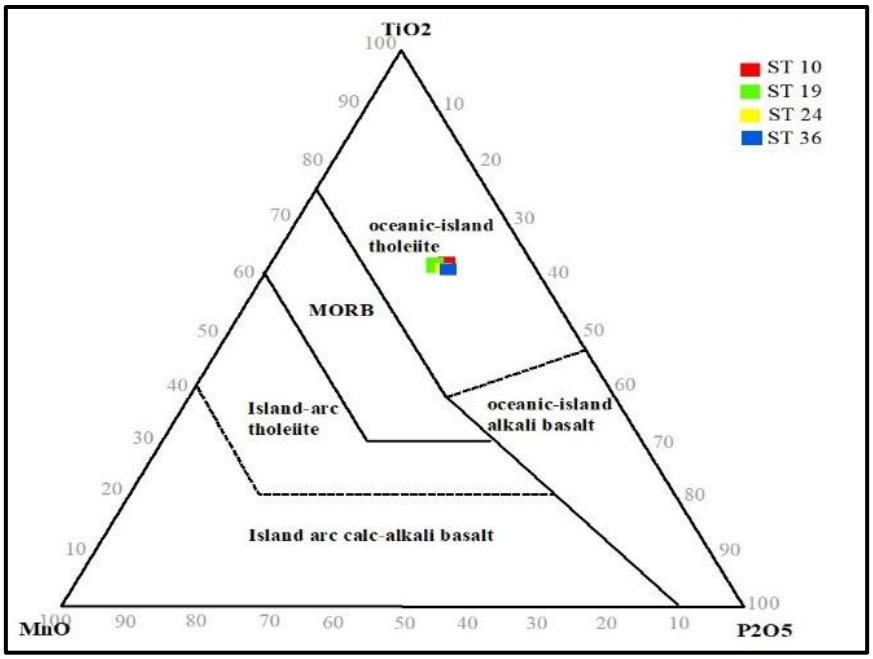


**Figure 8.** Plotting results on the tectonic setting diagram (Mullen, 1983).

The OIT interpretation is consistent with the measured major element characteristics, particularly $TiO_2$ ~1 wt% and $P_2O_5$ ~0.40–0.43 wt%, coupled with very low $K_2O$, which aligns with tholeiitic ocean-island basalt signatures and supports an intraplate source influence (Mullen, 1983; Sun & McDonough, 1989; Kerr, 2014). In OIT systems, plume-influenced mantle sources can yield enriched incompatible element tendencies relative to depleted mid-ocean ridge basalt, and major element proxies (including Ti and P behavior) provide supportive, though not exhaustive, evidence in the absence of broader trace element datasets (Sun & Nesbitt, 1978; Sun & McDonough, 1989).

Importantly, the petrographic assemblage (plagioclase + diopside/augite + olivine) is compatible with oceanic tholeiitic basalts and does not require hydrous, arc-like mineralogies, providing an independent consistency check on the discrimination results (Mullen, 1983; Winter, 2014). Thus, the OIT inference is reinforced by a coherent agreement between mineralogical evidence, major element geochemical systematics, and the tectonic discrimination diagram.

Geodynamically, the occurrence of OIT-type tholeiitic basalt in North Taopa can be interpreted as an oceanic intraplate basaltic component that was later incorporated into the complex tectonic collage of Sulawesi through accretion and collision. This interpretation is consistent with regional models emphasizing suturing, microplate interactions, and the incorporation of oceanic fragments

(Hall & Wilson, 2000; Hamilton, 1979; Simandjuntak & Barber, 1996), and is compatible with the presence of ophiolite-related remnants and oceanic lithosphere fragments in the broader region (Coleman, 1977).

By establishing (i) basaltic rock type, (ii) low-K tholeiitic affinity with Fe-enrichment, and (iii) an OIT tectonomagmatic signature, this study provides a coherent first-order geochemical framework for the North Taopa basalt unit, serving as a baseline for future work integrating trace elements, isotopes, and expanded sampling to further resolve mantle source characteristics and tectonic evolution.

## 4. CONCLUSIONS

Basaltic rocks from the Taopa Utara area were consistently identified as porphyritic basalt based on their petrographic characteristics and major-element geochemistry. Thin-section observations revealed hypocrystalline–porphyritic textures with plagioclase phenocrysts and microlites accompanied by clinopyroxene (diopside/augite), olivine, and opaque minerals, indicating two-stage crystallization followed by rapid cooling during emplacement. The XRF major-oxide data place all samples in the basalt field and demonstrate a subalkaline, very low-K signature with low total alkalis. The combination of relatively elevated total iron and the AFM trend indicates a tholeiitic magma series with Fe-enrichment consistent with the fractional crystallization of Mg-rich phases. Tectonomagmatic discrimination using $TiO_2$–MnO–$P_2O_5$ supports an oceanic island tholeiite (OIT) affinity, suggesting an intraplate oceanic mantle contribution to the basalt generation. The exceptionally low CaO is interpreted to reflect strong Ca depletion, most plausibly linked to the early and/or extensive crystallization and separation of Ca-rich plagioclase. Overall, these results provide a first-order geochemical baseline for the Taopa Utara basalts and support future work using expanded sampling, trace elements, and isotopes to refine mantle-source and tectonic interpretations.

## 5. REFERENCES

Cao, L., Lü, C., He, X., Rawlinson, N., Hao, T., Widiyantoro, S., Supendi, P., Zhao, L., Yuan, H., Zhao, M., Qiu, X., Rafie, M. T., Alfian, A., & Sahara, D. P. (2024). Mantle flow induced by the interplay of downgoing slabs revealed by seismic anisotropy beneath the Sula Block in eastern Indonesia. *Journal of Geophysical Research: Solid Earth, 129*, e2023JB028110. https://doi.org/10.1029/2023JB028110

Coleman, R. G. (1977). *Ophiolites: Ancient oceanic lithosphere?* Springer-Verlag.

Doucet, L. S., Tetley, M. G., Li, Z.-X., Liu, Y., & Gamaleldien, H. (2022). Geochemical fingerprinting of continental and oceanic basalts: A machine learning approach. *Earth-Science Reviews, 233*, 104192. https://doi.org/10.1016/j.earscirev.2022.104192

Godang, S., Saputro, S. P., Li, H., Satyana, A. H., & Srichan, W. (2025). Geochemistry of the Adang Volcanics in Western Sulawesi: Unveiling the tectonic evolution of the opening of the Makassar Strait. *Solid Earth Sciences, 10*(1), 100228. https://doi.org/10.1016/j.sesci.2025.100228

Hall, R., & Wilson, M. E. J. (2000). Neogene sutures in eastern Indonesia. *Journal of Asian Earth Sciences, 18*(6), 781–808. https://doi.org/10.1016/S1367-9120(00)00040-7

Hamilton, W. (1979). *Tectonics of the Indonesian region* (U.S. Geological Survey Professional Paper 1078). U.S. Geological Survey.

Irvine, T. N., & Baragar, W. R. A. (1971). A guide to the chemical classification of the common volcanic rocks. *Canadian Journal of Earth Sciences, 8*(5), 523–548. https://doi.org/10.1139/e71-055

Kerr, A. C. (2014). Oceanic plateaus. In *Encyclopedia of Earth Sciences Series*. Springer.

Le Bas, M. J., Le Maitre, R. W., Streckeisen, A., & Zanettin, B. (1986). A chemical classification of volcanic rocks based on the total alkali–silica diagram. *Journal of Petrology, 27*(3), 745–750. https://doi.org/10.1093/petrology/27.3.745

Marfian, F., Permana, A. P., & Akase, N. (2023). Study of petrogenesis andesite rock in Bualemo Region, North Gorontalo Regency based on XRF geochemistry analysis. *Jambura Geoscience Review, 5*(1), 63–70. https://doi.org/10.34312/jgeosrev.v5i1.16941

Mullen, E. D. (1983). $MnO/TiO_2/P_2O_5$: A minor element discriminant for basaltic rocks of oceanic environments and its implications for petrogenesis. *Earth and Planetary Science Letters, 62*(1), 53–62. https://doi.org/10.1016/0012-821X(83)90070-5

Nakamura, K. (2023). Practical applications and limitations of basalt discrimination diagrams. *Big Earth Data, 7*(4), 1081–1093. https://doi.org/10.1080/20964471.2023.2235731

Oggier, F., Widiwijayanti, C., & Costa, F. (2023). Global volcanic rock classification of Holocene volcanoes. *Scientific Data, 10*, 422. https://doi.org/10.1038/s41597-023-02324-7

Paputungan, U., Permana, A. P., & Akase, N. (2025). Identifikasi kualitas batugamping berdasarkan analisis geokimia dan petrografi daerah Pilolodaa Provinsi Gorontalo. *Journal of Applied Geoscience and Engineering, 4*(1), 31–41. https://doi.org/10.37905/jage.v4i1.33607

Park, J., Lim, H., Myeong, B., Jang, Y.-Deuk, & Brenna, M. (2022). Basaltic cognate enclaves from Dokdo Island as a window for intraplate mafic alkaline OIB magma dynamics in a back-arc basin. *Contributions to Mineralogy and Petrology, 177*, 86. https://doi.org/10.1007/s00410-022-01951-4

Peccerillo, A., & Taylor, S. R. (1976). Geochemistry of Eocene calc-alkaline volcanic rocks from the Kastamonu area, northern Turkey. *Contributions to Mineralogy and Petrology, 58*(1), 63–81. https://doi.org/10.1007/BF00384745

Ratman, N. (1976). *Peta Geologi Lembar Toli-Toli, Sulawesi* [Geological map]. Pusat Penelitian dan Pengembangan Geologi.

Rasyid, F. F. F. A., Zainuri, A., & Kasim, M. (2022). Geologi wilayah Tapaluluo dan sekitarnya, Kabupaten Gorontalo. *Journal of Applied Geoscience and Engineering, 1*(1), 1–12. https://doi.org/10.34312/jage.v1i1.15502

Simandjuntak, T. O., & Barber, A. J. (1996). Contrasting tectonic styles in the Neogene orogenic belts of Indonesia. In R. Hall & D. Blundell (Eds.), *Tectonic evolution of Southeast Asia* (Geological Society Special Publication No. 106, pp. 185–201). Geological Society, London. https://doi.org/10.1144/GSL.SP.1996.106.01.12

Simanjuntak, A. V. H., Palgunadi, K. H., Supendi, P., Muksin, U., Gunawan, E., Widiyantoro, S., Rawlinson, N., Daryono, M. R., Daryono, D., Karnawati, D., Hanifa, N. R., Pratama, C., & Ida, R. (2024). The western extension of the Balantak Fault revealed by the 2021 earthquake cascade in the central arm of Sulawesi, Indonesia. *Geoscience Letters, 11*, 35. https://doi.org/10.1186/s40562-024-00353-7

Sompotan, A. F. (2012). *Struktur geologi Sulawesi*. Perpustakaan Sains Kebumian, Institut Teknologi Bandung.

Song, T., Hao, T., Zhang, J., Cao, L., & Dong, M. (2022). Numerical modeling of North Sulawesi subduction zone: Implications for the east–west differential evolution. *Tectonophysics, 822*, 229172. https://doi.org/10.1016/j.tecto.2021.229172

Sun, S.-S., & McDonough, W. F. (1989). Chemical and isotopic systematics of oceanic basalts: Implications for mantle composition and processes. In A. D. Saunders & M. J. Norry (Eds.), *Magmatism in the ocean basins* (Geological Society Special Publication No. 42, pp. 313–345). Geological Society, London. https://doi.org/10.1144/GSL.SP.1989.042.01.19

Sun, S.-S., & Nesbitt, R. W. (1978). Petrogenesis of Archaean ultrabasic and basic volcanics: Evidence from rare earth elements. *Contributions to Mineralogy and Petrology, 65*(3), 301–325. https://doi.org/10.1007/BF00375516

Surono, & Hartono, U. (2013). *Geologi Sulawesi*. LIPI Press.

Takaew, P., Xia, J. C., & Doucet, L. S. (2024). Machine learning and tectonic setting determination: Bridging the gap between Earth scientists and data scientists. *Geoscience Frontiers, 15*(1), 101726. https://doi.org/10.1016/j.gsf.2023.101726

Travis, R. B. (1955). Classification of rocks. *Quarterly of the Colorado School of Mines, 50*(1).

Vermeesch, P., & Pease, V. (2021). A genetic classification of the tholeiitic and calc-alkaline magma series. *Geochemical Perspectives Letters, 19*, 1–6. https://doi.org/10.7185/geochemlet.2125

Winter, J. D. (2014). *Principles of igneous and metamorphic petrology* (2nd ed.). Pearson.

Zhang, X., Huang, T.-N., Chung, S.-L., Maulana, A., Mawaleda, M., Tien, C.-Y., Lee, H.-Y., & Liu, P.-P. (2022). Late Eocene subduction initiation of the Indian Ocean in the North

Sulawesi Arc, Indonesia, induced by abrupt Australian plate acceleration. *Lithos, 422–423*, 106742. https://doi.org/10.1016/j.lithos.2022.106742

Zhang, X., Chung, S.-L., Tien, C.-Y., Maulana, A., Mawaleda, M., Lee, H.-Y., Liu, P.-P., & Xi, J. (2024). Mid-Cretaceous to early Eocene Neo-Tethyan subduction records in West Sulawesi, Indonesia. *Bulletin of the Geological Society of America, 136*(5–6), 2558–2567. https://doi.org/10.1130/B37038.1